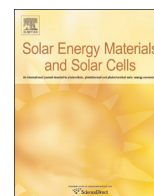




ELSEVIER

Contents lists available at ScienceDirect

Solar Energy Materials & Solar Cells

journal homepage: www.elsevier.com/locate/solmat

Angle resolved characterization of nanostructured and conventionally textured silicon solar cells



Rasmus Schmidt Davidsen^{a,*}, Jeppe Ormstrup^a, Martin Lind Ommen^a, Peter Emil Larsen^a, Michael Stenbæk Schmidt^a, Anja Boisen^a, Ørnulf Nordseth^c, Ole Hansen^{a,b}

^a Department of Micro- and Nanotechnology, Technical University of Denmark (DTU), Denmark

^b Danish National Research Foundation's Center for Individual Nanoparticle Functionality (CINF), Technical University of Denmark, DK-2800 Kgs. Lyngby, Denmark

^c IFE, Institute for Energy Technology, Norway

ARTICLE INFO

Article history:

Received 13 December 2014

Received in revised form

2 March 2015

Accepted 1 April 2015

Keywords:

Black silicon

Reactive ion etching

Incident angle

Reflectance

Angle-resolved characterization

ABSTRACT

We report angle resolved characterization of nanostructured and conventionally textured silicon solar cells. The nanostructured solar cells are realized through a single step, mask-less, scalable reactive ion etching (RIE) texturing of the surface. Photovoltaic properties including short circuit current, open circuit voltage, fill factor (FF) and power conversion efficiency are each measured as function of the relative incident angle between the solar cell and the light source. The relative incident angle is varied from 0° to 90° in steps of 10° in orthogonal axes, such that each solar cell is characterized at 100 different angle combinations. The angle resolved photovoltaic properties are summarized in terms of the average, angle-dependent electrical power output normalized to the power output at normal incidence and differently textured cells on different silicon substrates are compared in terms of angle resolved performance. The results show a 3% point improvement in average electrical power output normalized with respect to normal incidence power output of RIE textured, multicrystalline Si cells compared to conventional multicrystalline Si cells and above 1% point improvement of RIE textured monocrystalline Si cells compared to conventional monocrystalline Si cells.

© 2015 Elsevier B.V. All rights reserved.

1. Introduction

Solar cells are generally characterized at standard test conditions i.e. at light intensity of 1000 W/m², AM1.5G¹ illumination, temperature of 25 °C and light at normal incidence, which means that the incident simulated sunlight beam is directed at an angle of 90° relative to the solar cell plane. However these conditions only represent a very limited fraction of actual, realistic operating conditions for solar cells and panels. The temperature of the cell and the intensity and incidence angle of the sunlight indeed vary between different geographical locations and throughout the duration of a day and a year. Furthermore solar cells are subject to diffuse light whenever clouds, dust or any obstacles in the air scatter the sunlight before it reaches the solar cell surface. For this reason there is a need for a more detailed characterization scheme for solar cells, which takes these variations into account. In particular when considering alternative solar cell types employing

features such as nanoscale texturing of the solar cell surface, the angle-resolved and low light performance becomes more important, since nanoscale texturing has been shown [1–3] to yield superior reflectance properties over a broad range of incident angles compared to conventionally textured solar cells.

We use black silicon (BS) [4,5] nanostructuring to achieve low reflectance due to the resulting graded refractive index at the Si–air interface. Low broadband reflectance at different incident angles has been reported for moth-eye surfaces [6,7] and different types of black silicon [8] are fabricated by means of various methods. This work focuses on black Si fabricated by maskless reactive ion etching (RIE). Repo et al. [9] achieved a power conversion efficiency of 18.7% on 400 μm thick float-zone Si using cryogenic deep RIE as texturing and plasma assisted atomic layer deposition (ALD) of Al₂O₃ for a passivated emitter rear locally diffused (PERL) cell. Oh et al. [3] achieved a power conversion efficiency of 18.2% on 300 μm thick float-zone Si by combining a metal-assisted wet etching black silicon process for texturing, TMAH damage removal etch and double-sided thermal SiO₂ passivation. Yoo [10] used industry grade Czochralski Si and RIE texturing and achieved a power conversion efficiency of 16.7%. Several groups have reported improved light absorption over a broad range of incident angles of nanostructured [11–14] and

* Correspondence to: Ørsted Plads building 345 East, 2800 Lyngby, Denmark, E-mail address: rasda@nanotech.dtu.dk (R.S. Davidsen).

¹ AM1.5G=Air Mass of 1.5 Global.

differently textured Si including the PERL-cell [15,16]. Considering these reported improved angle-dependent optical properties of nanostructured Si and the correlation between overcast sky (diffuse light) conditions and relative incident angle of the sunlight [17–20], the relationship between nanostructured Si solar cells and angle-dependent photovoltaic performance is of utmost interest with respect to optimization of solar cell performance under realistic operating conditions such as diffuse light. Lee et al. [21] show improved average power conversion efficiency as function of incident angle of nanostructured thin film Si solar cells in comparison with “conventional” thin film Si cells with single and double anti-reflective (AR) coatings. However, a detailed study of the angle-dependent photovoltaic performance of nanostructured, large-area Si solar cells based on industrial type Si substrates in direct comparison with conventionally textured Si solar cells, has not yet been reported.

This work presents an angle-resolved characterization approach of solar cells in general and measured angle-resolved photovoltaic properties of nanostructured Si solar cells in comparison with conventionally textured Si solar cells.

2. Approach

The maskless RIE process presented in this work is applied as the texturing step in the following solar cell fabrication process:

- Saw damage removal by etching in 30% KOH at 75 °C for 2 min and subsequent cleaning in 20% HCl at room temperature for 5 min and rinsing in deionized water.
- Texturing using maskless RIE at room temperature in a O₂ and SF₆ plasma with a gas flow ratio of O₂:SF₆ ≈ 1:1, chamber pressure of 28 mTorr, 13.56 MHz radio-frequency platen power of 30 W using a STS RIE system.
- Emitter formation using a tube furnace from Tempres Systems with liquid POCl₃ as dopant source and N₂ as carrier gas at a temperature of 840 °C and atmospheric pressure for 50 min in O₂ ambient, followed by removal of phosphor-silicate glass (PSG) in 5% hydrofluoric acid (HF).
- Plasma enhanced chemical vapour deposition (PECVD) of 60 nm hydrogenated amorphous silicon nitride (SiN_x:H) anti-reflective coating at 400 °C using a PlasmaLab System133 from Oxford Instruments.
- Screen-printing of Ag front and Al rear contacts with standard Ag and Al pastes using an Ekra X5-ST5 screen printer, followed by co-firing of the front and rear contacts at 800 °C using an RTC Model LA-309 belt furnace.
- Edge isolation by laser ablation using a J-1030-515-343 FS System from Oxford Lasers Ltd.

The starting substrates were 156 × 156 mm² p-type, CZ mono-, multi- and quasi-mono-crystalline Si wafers with a thickness of 200 μm and a resistivity of 1–3 Ω cm.

3. Characterization

Normal incidence reflectance measurements of the RIE-textured mono-, multi and quasi-mono Si surfaces were performed using a broadband lightsource (Mikropack DH-2000), an integrating sphere (Mikropack ISP-30-6-R), and a spectrometer (Ocean Optics QE65000, 280–1000 nm). The reference solar spectral irradiance for AM1.5 was used to calculate the weighted average reflectance in the wavelength range from 280 to 1000 nm. The angle-dependent optical reflectance was measured with monochromatic light from 350 nm to 1200 nm using an APEX monochromator illuminator with an Oriel Cornerstone

260 1/4 m monochromator. A quartz crystal achromatic depolarizer from Thorlabs was used in the beam path to randomize the partly polarized light from the monochromator. The sample was inserted inside a 150 mm integrating sphere with a centre mount configuration and rotated to any desired angle of incidence.

I–*V* curves and photovoltaic properties including short-circuit current, *I*_{SC}, open-circuit voltage, *V*_{OC}, fill factor, FF, and electrical output power, *P*_{el}, were measured on complete cells under 1 sun illumination (1000 W/m², AM1.5G) using a Newport Oriel 92190 large-area Xe light source and a Keithley 2651A high-power source meter.

In order to characterize the solar cell performance at varying incident angles, *I*–*V* curves were measured on differently textured Si solar cells mounted and contacted on a stage, which prior to each *I*–*V* curve measurement was tilted to a position given by two angles, θ and ϕ , around two orthogonal axes: θ is the tilt of the cell plane with respect to the original, horizontal x-axis and ϕ is the tilt of the cell plane with respect to the tilted y-axis. The light source was fixed during all measurements. The measurement setup including the two angles θ and ϕ is sketched in Fig. 4. The incidence angle was varied using two JVL QuickStep stepping motors connected to the solar cell stage. Each angle was randomly varied in steps of 10° in the range 0–90° unless otherwise specified. At each angle combination, (θ , ϕ), the *I*–*V* curve was measured under 1 sun and the result collected using LabView, such that a total of 100 *I*–*V* curves were measured for each cell. The measured *I*–*V* curves were then analysed in order to determine *I*_{SC}, *V*_{OC}, FF and *P*_{el} at each angle combination, (θ , ϕ), using SciLab. Finally the angle-resolved photovoltaic properties were plotted and the average electrical power output normalized to the normal incidence power output was calculated in order to compare the angle-dependency of different cells. A LEO 1550 Scanning Electron Microscope (SEM) was used to characterize the nanostructured surface topology.

4. Results

An example of the nanostructured surfaces realized by maskless RIE in this work is seen in Fig. 1.

The nanostructures seen in Fig. 1 are conical-like hillocks randomly distributed across the entire solar cell surface. The nanostructures are on average 300–400 nm tall with an area density of ~100 μm⁻². The topology is shown with and without ~60 nm PECVD SiN_x:H in Fig. 1. It is seen from Fig. 1(a) that the SiN_x:H AR-coating does not change the RIE-textured topology significantly, but makes the nanostructure edges slightly more round and smooth.

Fig. 2 shows total weighted average reflectance of RIE-textured Si below 1.1% for all three crystalline grades of Si, which is a clear improvement compared to KOH- and acidic-textured Si used in standard industrial Si solar cells. With anti-reflective coating KOH-textured Si has reflectance of 2% [22], while acidic-textured multi-crystalline Si has reflectance of 8% [23]. It is seen that the average reflectance is unaffected by the ~60 nm PECVD SiN_x:H AR-coating. The results furthermore show negligible increase in reflectance after emitter diffusion. The RIE-textured Si shows ~0.1% minimum reflectance independent of crystalline grade. The power conversion efficiencies at normal incidence of the fabricated solar cells are summarized in Table 1. Table 1 shows that the RIE-textured cells have lower power conversion efficiency than the conventionally textured cells primarily due to lower short-circuit current, but also reduced open-circuit voltage. Based on IQE-measurements and LASSIE² analysis, the current and voltage losses were explained by increased emitter and surface

² Loss analysis of silicon solar cells by IQE evaluation.

Download English Version:

<https://daneshyari.com/en/article/6535158>

Download Persian Version:

<https://daneshyari.com/article/6535158>

[Daneshyari.com](https://daneshyari.com)